

WavePacket: A Matlab package for numerical quantum dynamics.

II: Open quantum systems, optimal control, and model reduction

Burkhard Schmidt*

Institut für Mathematik, Freie Universität Berlin

Arnimallee 6, D-14195 Berlin, Germany

Carsten Hartmann[†]

Institut für Mathematik, Brandenburgische Technische Universität

Konrad-Wachsmann-Allee 1, D-03046 Cottbus, Germany

(Dated: February 23, 2022)

Abstract

WavePacket is an open-source program package for numeric simulations in quantum dynamics. It can solve time-independent or time-dependent linear Schrödinger and Liouville-von Neumann equations in one or more dimensions. Also coupled equations can be treated, which allows, e.g., to simulate molecular quantum dynamics beyond the Born-Oppenheimer approximation. Optionally accounting for the interaction with external electric fields within the semi-classical dipole approximation, WavePacket can be used to simulate experiments involving tailored light pulses in photo-induced physics or chemistry. Being highly versatile and offering visualization of quantum dynamics 'on the fly', WavePacket is well suited for teaching or research projects in atomic, molecular and optical physics as well as in physical or theoretical chemistry. Building on the previous Part I [Comp. Phys. Comm. **213**, 223-234 (2017)] which dealt with closed quantum systems and discrete variable representations, the present Part II focuses on the dynamics of open quantum systems, with Lindblad operators modeling dissipation and dephasing. This part also describes the WavePacket function for optimal control of quantum dynamics, building on rapid monotonically convergent iteration methods. Furthermore, two different approaches to dimension reduction implemented in WavePacket are documented here. In the first one, a balancing transformation based on the concepts of controllability and observability Gramians is used to identify states that are neither well controllable nor well observable. Those states are either truncated or averaged out. In the other approach, the H2-error for a given reduced dimensionality is minimized by H2 optimal model reduction techniques, utilizing a bilinear iterative rational Krylov algorithm.

The present work describes the MATLAB version of WavePacket 5.3.0 which is hosted and further developed at the Sourceforge platform, where also extensive Wiki-documentation as well as numerous worked-out demonstration examples with animated graphics can be found.

PACS numbers:

Keywords:

*Electronic address: burkhard.schmidt@fu-berlin.de

†Electronic address: carsten.hartmann@b-tu.de

Program Summary

Program Title

WAVEPACKET

Licensing provisions

GPLv3

Programming language

MATLAB

Journal reference of previous version

Comput. Phys. Comm. **213** (2017), 223.

Does the new version supersede the previous version?

The previous article focused on the treatment of closed quantum systems by discrete variable representations and implementation of various numerical algorithms for solving Schrödinger's equations. Complementary to that, the present second part is concerned with open quantum systems and optimal control by external fields. In addition, two approaches to dimension reduction useful in modeling of quantum control are described.

Reasons for the new version

The reason for having a second article on the WavePacket software package lies in the fact that a complete description of the package would have exceeded the scope of a regular article. Several significant features of the WAVEPACKET package are introduced here which could not be mentioned in the first article, due to length constraints.

Summary of revisions

Here we describe the numerical treatment of open quantum systems dynamics modeled by Lindblad master equations. Moreover, we explain the WAVEPACKET functions for optimal control simulations, both for closed and open quantum systems. To address the problem of computational effort, two strategies for model reduction have been included.

Nature of problem

Dynamics of closed and open systems are described by Schrödinger or Liouville-von Neumann equations, respectively, where the latter ones will be restricted to the Lindblad master equation. Emphasis is on the interaction of quantum system with external electric fields, treated within the semi-classical dipole approximation. Quantum optimal control simulations are used for the design of tailored fields achieving specified targets in quantum dynamics. With these features, WAVEPACKET can be instrumental for the simulation, understanding, and prediction of modern experiments in atomic, molecular and optical physics involving temporally shaped fields.

Solution method

Representing state vectors or reduced density matrices in a discrete basis, Schrödinger or Liouville-von Neumann equations are cast into systems of ordinary differential equations. Those are treated by self-written or MATLAB's built-in solvers, the latter ones offering adaptive time-stepping. The optimal control equations are solved by the rapid monotonically convergent iteration methods developed by Zhu, Rabitz, Ohtsuki and others. In order to reduce the dimensionality of large scale control problems, the balanced truncation method as well as H2-optimal model reduction approaches are available in WAVEPACKET.

Additional comments including restrictions and unusual features

The WAVEPACKET program package is rather easy and intuitive to use, providing visualization of quantum dynamics 'on the fly'. It is mainly intended for low-dimensional systems, typically not exceeding three to five degrees of freedom. Detailed user guides and reference manuals are available through numerous Wiki pages hosted at the SOURCEFORGE platform where also a large number of well documented demonstration examples can be found.

I. INTRODUCTION

The evolution of ultrafast experimental techniques, mainly triggered by advances in generating short intense laser pulses in the late 20th century, has been a strong motivation for studying quantum mechanics also from the time-dependent point of view [1–3]. Nowa-

days, experiments using tailored laser fields are often accompanied by quantum dynamical simulations resulting in substantial progress in the fields of atomic and molecular physics [2, 4], femtochemistry [3, 5] and even femtobiology [6]. Concepts developed in these fields are also instrumental in quantum information theory; for approaches to quantum computing in molecular physics see, e. g. Refs. [7–9]. It can be expected that the control of quantum systems may lead to a variety of potential quantum technologies in the future [10].

Despite of the obvious importance of quantum dynamical simulations, general-purpose and freely available simulation software is still rather scarce; notable exceptions being the MCTDH program package which specializes in weakly coupled, high-dimensional systems [11], or the nearly linearly scalable TDDVR package [12], both of which are mainly used in the context of quantum molecular dynamics. Other software packages more commonly used in the physics community include QUTIP for the dynamics of open quantum systems [13, 14], the FERMIFAB toolbox for many-particle quantum systems [15], and the QLIB platform for numeric optimal control [16].

In this work we continue the description of the MATLAB version of our WAVEPACKET software for numeric quantum dynamics which we decided to split into two articles, due to length constraints. In Part I we have introduced this general software package, with regard to its use for closed quantum systems [17], i. e., mainly the solution of Schrödinger equations (SE). These parts of WAVEPACKET are based on describing wave functions and operators in finite basis representations (FBRs) and/or associated discrete variable representations (DVRs) [18, 19]. This FBR/DVR approach allows to cast the time-independent Schrödinger equation (TISE) into an eigenvalue problem which is solved by the WAVEPACKET function `qm_bound`. In close analogy, the time-dependent Schrödinger equation (TDSE) is solved in a partial differential equation (PDE) setting by a variety of propagation methods implemented in the function WAVEPACKET `qm_propa`. The efficiency of both approaches relies on fast transformations between DVRs and FBRs, the most prominent example of which being fast Fourier transforms for use with plane wave FBRs [20]. Finally, among the WAVEPACKET functions introduced in Part I there is also a visualization tool `qm_movie` which can be used to generate different types of animated graphics, as well as the auxiliary functions `qm_setup` and `qm_cleanup` to initialize and finalize simulation protocols.

Another emphasis of Part I is on the manipulation of quantum systems by external electric fields. The interactions are treated within the framework of the semi-classical dipole

approximation, hence making WAVEPACKET especially suitable for simulating experiments in photophysics or photochemistry where shaped field pulses are used to alter, and ultimately to control, the dynamics of quantum systems. Yet another feature of WAVEPACKET is that it can treat coupled (multi-channel) SEs occurring, e. g., for systems with slow and heavy degrees of freedom, such as nuclei and electrons in molecular systems. Using WAVEPACKET, the quantum dynamics of such systems can be treated beyond the Born-Oppenheimer (adiabatic) approximation, including situations where the dynamics is typically dominated by non-adiabatic transitions occurring near (avoided) crossings or conical intersections of potential energy curves or surfaces, respectively [21, 22].

The present, complementary Part II extends the previous work of Ref. [17] by describing the use of WAVEPACKET for simulations of open quantum systems modeled in terms of Liouville-von Neumann equations (LvNE) [23, 24]. Here, we will restrict ourselves to Lindblad-Kossakowski models for dissipation and dephasing of quantum systems interacting with a thermal bath [25, 26]. In order to treat closed and open quantum systems on an equal footing, it is advantageous to change from DVR ("coordinate") and/or FBR ("momentum") representations to an eigen ("energy") representation. Then the corresponding equations of closed (TDSE) and open (LvNE) systems become sets of coupled ordinary differential equations (ODEs). In fact, all WAVEPACKET functions introduced in the present Part II are based on an energy representation in terms of eigenenergies and eigenfunctions which can be obtained, e. g. using `qm_init` and `qm_bound`, see Secs. II and III. The further course of a typical workflow is shown in the flow chart in Fig. 1. Within WAVEPACKET, the actual change of representation is carried out in our function `qm_matrix`, see Sec. IV. This is followed by function `qm_abncd` which sets up the ODE formulations of the TDSE or the LvNE. In doing so, we make use of the fact that quantum dynamics of driven systems within the semi-classical dipole approximation displays many formal analogies with control theory of bilinear systems. Note that the name `qm_abncd` alludes to the usual convention of denoting the system matrices as A, B, N, C, D , see Sec. V.

Once the system matrices have been set up, the TDSEs or the LvNEs are solved numerically by using conventional ODE solvers, which is realized in our code `qm_control` described in Secs. VI. Moreover, since version 5.2.0 released in 2016, also optimal control techniques have been implemented in WAVEPACKET where the time-dependence of optimal control fields is determined automatically, striving at optimizing certain user-defined control targets

[27–29], often subject to constraints arising due to laboratory technologies. Typical examples for such constraints are limitations in the intensity of available light pulses. With our function `qm_optimal` described in Sec. VII, we present a code for optimization of various types of targets, subject to field constraints, which builds on the rapidly converging methods introduced in Refs. [30–35]. Due to the general formulation in terms of the system matrices used in control theory, the WAVEPACKET function `qm_optimal` can be used both for closed and open quantum systems, or even for control problems from completely different sources, e. g. classical Langevin dynamics [36] or Fokker-Planck dynamics [37].

The main obstacle when simulating the control of multi-dimensional quantum systems is the exponential growth of the number of quantum states with the number of the degrees of freedom. Even for relatively small systems, this can lead to an exceedingly high computational effort, especially for open quantum systems (LvNE) dynamics where the size of the system matrices scales quadratically with the number of quantum states involved, which makes dimension reduction highly desirable. For such cases, WAVEPACKET offers a balancing transformation reconciling the concepts of controllability and observability [38]. As described in Sec. VIII, the function `qm_balance` aims at constructing states which are both controllable and observable. The remaining states, i. e. those which are neither well controllable nor well observable, do not contribute notably to the input-output behavior of a control system. Hence, the WavePacket function `qm_truncate` can be used to eliminate those states, see Sec. IX. This is either achieved by a simple truncation or, in analogy with systems displaying fast and slow degrees of freedom, by averaging them out, based on singular perturbation theory [37, 39, 40]. An alternative approach to model reduction will be given in Sec. X. The function `qm_reduce` serves to minimize the residual \mathcal{H}_2 -error quantifying the deviation between the full system and a system of (given) reduced dimensionality, utilizing a bilinear iterative rational Krylov algorithm [37, 41, 42].

II. QM_INIT

A. Initialize WavePacket simulations

For any WAVEPACKET simulation, the structure of the quantum-mechanical Hamiltonian operator must be of the form introduced in Part I

$$\hat{H}(\hat{R}, -i\nabla_R, t) = \hat{T}(\hat{R}, -i\nabla_R) + \hat{V}(\hat{R}) - F(t) \cdot \hat{\mu}(\hat{R}) \quad (1)$$

where \hat{T} and \hat{V} are kinetic and potential energy operators, respectively. They are expressed in terms of position and momentum operators, \hat{R} and $-i\nabla_R$, which can be in one or more dimensions. The dynamics of the quantum system can be controlled by electrical field components $F_k(t)$ with $k \in \{x, y\}$ allowing to account for different polarization directions. Within the semi-classical dipole approximation they interact with the quantum system through its dipole moment components $\mu_k(\hat{R})$. Note that the induced dipole interaction involving products of the polarizabilities and the field squared has been omitted here because it is not yet implemented in all the codes described below. The same holds for (optional) negative imaginary potential, which can be used to absorb wavefunctions near the boundaries. For the description of open quantum systems we employ a simple model of the system–bath coupling (SBC) Hamiltonian. Its dependence on the system’s degrees of freedom is modeled by functions $\chi(R)$ while the dependence on the bath modes \hat{r}_β is assumed to be linear

$$\hat{H}_{\text{SB}} = \sum_{\beta} \chi_{\beta}(\hat{R}) \hat{r}_{\beta} \quad (2)$$

where the summation extends over all bath modes β . For more details, see Sec. V and appendix B.

It is emphasized that WAVEPACKET can also be used to solve coupled Schrödinger equations in which case \hat{H} is an operator matrix and the potential \hat{V} as well as the dipole moments $\hat{\mu}_k$ become matrix-valued. This occurs, e. g., for systems comprising of heavy and light particles, where \hat{R} and $-i\nabla_R$ refer to the former ones, while the matrices of \hat{V} and $\hat{\mu}_k$ refer to the quantization of the latter ones.

Within WAVEPACKET, all settings concerning the Hamiltonian (1) have to be specified by the user. Most conveniently this can be achieved with a user-defined function, which we recommend to name `qm_init`. Typically such a function will also contain further settings,

in particular those required for the discrete variable representations (DVRs) and/or the corresponding finite basis representations (FBRs). Those representations are underlying the functions `qm_bound` as well as `qm_propa`, both of which are described in great detail in Part I. However, for completeness, the former one will be shortly reviewed in the following Sec. III, before switching from DVR / FBR to energy representations in Sec. IV.

B. Example: Morse oscillator in FFT grid representation

We first choose the rather simple example system of a Morse oscillator already introduced in Part I; generalizations to more dimensions and/or more complex scenarios can be found in the demo examples available in the Wiki documentation of WAVEPACKET at SOURCEFORGE. We consider a one-dimensional Morse potential with dissociation energy D_e , equilibrium position R_e , and range parameter $\alpha > 0$, the values of which are chosen to resemble an OH oscillator inside a water molecule in its electronic ground state [30, 31, 43]. The Morse system interacts with an external electric field through a dipole moment modeled by a Mecke function [44] with charge and distance parameters $R_0 = 0.6 \text{ \AA}$ and $q_0 = 7.85 \text{ D/\AA}$, respectively. For the case of open quantum systems, the R -dependence of the system-bath coupling, $\chi(R)$, see Sec. V and appendix B, is modeled by a linear function with slope one for simplicity.

The necessary settings of the MATLAB function `qm_init` could read as follows

```
global atomic hamilt space

hamilt.pot.handle = @pot.morse;
hamilt.pot.d_e = 0.1994;
hamilt.pot.r_e = 1.821;
hamilt.pot.alf = 1.189;

hamilt.dip.handle = @dip.mecke;
hamilt.dip.r_0 = 0.6/atomic.l.A;
hamilt.dip.q_0 = 7.85/atomic.d.D*atomic.l.A;
```

```

hamilt.sbc.handle = @sbc.taylor;
hamilt.sbc.v{1,1} = 1;

space.dof{1} = grid.fft;
space.dof{1}.mass = 0.9481/atomic.m.u;
space.dof{1}.n_pts = 256;
space.dof{1}.x_min = 0.7;
space.dof{1}.x_max = 10.0;

```

The first line makes the three global variables available inside the function. Note that it is a general feature of the Matlab version of WavePacket to use few, but highly structured variables to simplify book-keeping and to avoid passing values of arguments between functions as is required in some older versions of Matlab.

The choices of the Morse potential, the Mecke dipole function, and the linear system bath coupling (Taylor series with first term only) are realized through function handles, i.e., references to functions located within the package folders `+pot`, `+dip`, `+sbc`, respectively. The choice of the FFT-based plane wave FBR is realized by constructing an object pertaining to one of the MATLAB classes in folder `+grid`. The `fft` class used here requires the reduced mass, the number of grid points as well as the lower and upper bounds of the grid to be specified.

The use of function handles and grid classes allows easy customization since WAVEPACKET comes with a large number of built-in models, see the Reference Manual on our Wiki pages. In addition, there is the possibility for the user to supply custom functions and/or classes. As an alternative, the necessary functions can also be specified in terms of a Taylor series, or they can be given as tabulated values from formatted data files, which are then interpolated.

Throughout the WAVEPACKET software package, atomic units are used, where Planck's constant \hbar , the electronic mass m_e and the elementary charge e are scaled to unity. However, conversions from and to SI (and other frequently used) units are provided through the fields of global variable `atomic` as can be seen in some of the sample code lines above. Note that also the most important isotopic masses of frequently encountered atom types are available there. In principle, the sample code lines given above are equivalent to those given as an

example in Part I. However, for a few minor syntax changes, see Appendix A.

C. Workflow

Once, the initialization function `qm_init` has been set up, a typical workflow for a WAVEPACKET simulation could be as follows

```
qm_setup;
qm_init;
qm_bound;
qm_cleanup
```

where the function `qm_bound` for bound state calculations can be exchanged by any of the functions described in the following sections. For more details of the workflow, as well as the possibilities of more sophisticated MATLAB scripts, the reader is referred to Sec. 2 of Part I.

III. QM_BOUND

A. Calculation of bound states

Once the Hamiltonian, along with the necessary DVR and FBR schemes, is specified in `qm_init`, the time-independent Schrödinger equation (TISE)

$$\hat{H}_0(R, -i\nabla_R)\Psi_j(R) = E_j\Psi_j(R) \quad (3)$$

can be solved. Here E_j and $\Psi_j(R)$ are the eigenvalues and eigenfunctions of $\hat{H}_0 = \hat{T} + \hat{V}$ which equals the Hamiltonian of Eq. (1) but without the last (time-dependent) term. As explained in detail in Part I, the default method to solve the TISE numerically within WAVEPACKET is by direct diagonalization using `qm_bound` which is based on DVR and FBR methods. The numerical solutions are restricted to the calculation of bound states; calculations of scattering states are planned for future versions of our software package.

In any simulation using `qm_bound` (as well as `qm_propa` for time-dependent simulations), expectation values of positions, momenta, and energies are routinely monitored. Moreover,

WAVEPACKET offers the possibility to calculate time-independent (or time-dependent) expectation values of additional multiplicative operators (AMOs). For example, in simulations of molecular rotation the degree of orientation and/or alignment can be determined as mean values of $\cos \theta$ or $\cos^2 \theta$, respectively, where θ is the angle between the axis of the molecule and the polarization of the external field [45, 46]. In simulations of chemical reaction dynamics, projecting on the reactant and/or the product space can be instrumental in monitoring reaction probabilities [47]. So far, these possibilities are restricted to AMO operators which are multiplicative in position representation (DVR). For future versions, we plan also additional differential operators (ADOs), i. e., operators which are multiplicative in momentum representation (FBR).

B. Example: Morse oscillator bound states

Here we return to the example of the Morse oscillator and add a few lines to the WAVEPACKET initialization function `qm_init` to define an AMO

```
space.amo{1}.handle = @amo.gauss;
space.amo{1}.pos_0 = 2.5;
space.amo{1}.width = 1/50;
```

Here the function handle in the first code line indicates that we have chosen a Gaussian function which can be used as a target in (optimal) control of molecular bond length [31], see Sec. VII. The corresponding MATLAB function `gauss.m` is located in the `+amo` package folder in the source code directory, along with a few other model functions. Again, it is emphasized that such functions can be easily provided by the user, in order to adapt WAVEPACKET to specific simulation requirements. It is also possible to specify more than one additional multiplicative operator in which case the indices inside the curly braces have to be set appropriately.

Furthermore, it is possible to specify that all 22 bound states of the OH Morse oscillator with $0 \leq v \leq 21$ are to be visualized and their expectation values to be included in the logfile output which can be achieved by adding the following lines to `qm_init`

```
global psi
psi.eigen.stop = 0;
```

```
psi.eigen.stop = 21;
```

Note that a Wigner representation of the highest bound state of our Morse oscillator is shown in Fig. 4 of Part I.

Another recommended option is to store the calculated wave functions which is triggered by two more lines in `qm_init`

```
psi.save.export = true;
psi.save.file = 'bound';
```

Here the last line indicates that the wave functions are to be stored in unformatted MATLAB data files `bound.mat`, `bound_0.mat`, These files serve not only as an input to the visualization function `qm_movie` described in Sec. 6 of Part I, but they also provide the necessary data for `qm_matrix`, see the following section.

IV. QM_MATRIX

A. From coordinate to energy representation

Once the time-independent Schrödinger equation (3) has been solved for using DVR / FBR techniques, the function `qm_matrix` can be used to set up an energy representation in terms of the obtained eigenenergies, E_j , and eigenfunctions, $\Psi_j(R)$, of the field-free Hamiltonian $\hat{H}_0 = \hat{T} + \hat{V}$. The resulting change from PDEs to coupled ODEs makes it easier to set up the equations of motion for closed and open quantum systems on an equal footing, see Sec. V.

Within the `WAVEPACKET` function `qm_matrix`, the change from DVR (coordinate) and/or FBR (momentum) to energy (or eigen) representation is achieved by calculating matrix elements of the dipole operator

$$\mu_{ij}^{(k)} = \langle i | \mu_k | j \rangle = \int dR \Psi_i^*(R) \mu_k(R) \Psi_j(R) \quad (4)$$

where $k \in \{x, y\}$ allows to simulate the interaction with light of different polarization directions. For open quantum systems, `qm_matrix` similarly evaluates matrix elements of the system-bath coupling, $\chi(R)$, see Eq. (2) and appendix B. All integrals are obtained by means of the numerical quadratures underlying the DVRs; for details see Sec. 3.3 of Part I.

Moreover, the function `qm_matrix` serves to generate energy representations of observables used as control targets in the (optimal) control functions described in the following sections. Currently, there are three options available:

- Additional multiplicative operators (AMOs) as introduced in Sec. III. The matrix elements of \hat{O}_q are given by

$$O_{ij}^{(q)} = \langle i | \hat{O}_q | j \rangle \quad (5)$$

where again the required integrals are calculated by DVR quadratures.

- Populations of (one or more) selected eigenstates. The matrix elements of the corresponding projectors \hat{P}_q are given by

$$P_{ij}^{(q)} = \langle i | \hat{P}_q | j \rangle = \langle i | q \rangle \langle q | j \rangle \quad (6)$$

in which case the only non-zero matrix elements are ones on the appropriate (q -th) position(s) along the main diagonal.

- Alternatively, populations can be obtained as squared moduli of overlaps with eigenstates which are simply given as a vector with elements

$$\Pi_i^{(q)} = \langle i | q \rangle = \delta_{i,q} \quad (7)$$

where the only non-zero elements are ones on the appropriate (q -th) position(s).

Even though the latter two options are formally equivalent, there are non-trivial differences when using them as targets in numeric optimal control simulations, see Sec. VII C.

All matrix elements of the dipole operators (4), system bath couplings, as well of those of one of the three classes of observables (5-7) are written to an unformatted MATLAB data file named `tise.mat`. Alternatively, these data may also come from other sources outside WAVEPACKET. For example, in simulations of electronic dynamics of atomic or molecular systems, the necessary matrix elements can be generated by quantum chemical (electronic structure) calculations.

B. Morse oscillator matrix elements

Here we return to the example of the Morse oscillator already used in the previous sections. Because its spectrum also contains a continuum of scattering states, the transforma-

tion of quantum dynamics from a DVR/FBR to an energy representation leads to integro-differential equations also accounting for the bound-continuum coupling [43]. However, this coupling can be neglected as long as frequencies and/or intensities of the control fields are not too high, in which case the study of vibrational excitation of a Morse oscillator can still be pursued in an ODE setting. Otherwise, one would have to resort to numerical techniques for the discretization of a quasi-continuum [48] which have been used, e. g. in modeling dissociation or ionization spectroscopy [49]. However, those approaches are currently not yet implemented in WAVEPACKET.

When using the Gaussian-shaped AMO introduced in Sec. IIIB as control target, the following lines have to be added to the WAVEPACKET initialization function `qm_init.m`

```
global control
control.observe.targets = 'amo';
control.observe.choices = {1};
```

If more than one AMO has been specified before, several indices could be given in the cell vector on the r.h.s. of the latter code line.

Alternatively, the choice of bound state populations as control targets is specified as follows

```
control.observe.types = 'prj';
control.observe.choices = {[0] [1] [2] [3] [4] [5:10] [11:21]};
```

where five single states and two groups of states are given here for illustration. The above mentioned possibility of using (squares of) overlaps instead of projectors when using populations as control targets is selected by specifying 'ovl' instead of 'prj' above.

V. QM_ABNCD

A. From closed to open quantum systems

The function `qm_abnacd` is intended to set up simulations of closed and open quantum systems using a common framework in terms of A, B, N, C, D matrices frequently used in the literature on control systems, see Secs. VB and VC below. The evolution of a closed

non-relativistic quantum system is described in terms of the time-dependent Schrödinger equation (TDSE)

$$i\frac{d}{dt}|\Psi(t)\rangle = \hat{H}(\hat{R}, -i\nabla_R, t)|\Psi(t)\rangle, \quad |\Psi(t=0)\rangle = |\Psi_0\rangle \quad (8)$$

where the expectation values of the q -th observable \hat{O}_q are obtained as mean values

$$\langle \hat{O}_q \rangle(t) = \langle \Psi(t) | \hat{O}_q | \Psi(t) \rangle \quad (9)$$

While `qm_propa` can be used to solve the TDSE (8) in a PDE setting using DVR/FBR techniques as explained in Part I, the `WAVEPACKET` function `qm_abncd` sets up the ODE formulation in energy representation, based on the matrix elements obtained from `qm_matrix`, see Sec. IV.

Alternatively, function `qm_abncd` can be used to set up simulations of open quantum systems, i. e., systems thermally coupled to a heat bath [1, 23, 24]. Within the Lindblad formalism, the evolution of the reduced density operator ρ is governed by the following quantum master equation (Liouville-von Neumann equation, LvNE)

$$\frac{d}{dt}\hat{\rho} = -i \left[\hat{H}, \hat{\rho} \right]_- - \sum_{\ell} \left\{ \hat{L}_{\ell} \hat{\rho} \hat{L}_{\ell}^{\dagger} - \frac{1}{2} \left[\hat{L}_{\ell}^{\dagger} \hat{L}_{\ell}, \hat{\rho} \right]_+ \right\}, \quad \hat{\rho}(t=0) = \hat{\rho}_0 \quad (10)$$

where $[\cdot, \cdot]_-$ and $[\cdot, \cdot]_+$ stand for commutators and anticommutators, respectively. The first term of the r.h.s. of (10) is the Hamiltonian part describing the dynamics of a closed system. The second term represents the coupling to the environment, i. e., dissipation and/or dephasing. For the different choices of Lindblad operators \hat{L}_{ℓ} available inside `WAVEPACKET`, see appendix B. Within the LvNE setting, the time dependence of expectation values of observables can be calculated as

$$\langle \hat{O}_q \rangle(t) = \text{Tr}(\hat{O}_q \hat{\rho}(t)) \quad (11)$$

where Tr denotes the trace operation.

B. Input equations

In linear time-invariant (LTI) system theory [50] the input equation of a control system describes the evolution of its state vector $x(t) \in C^n$

$$\dot{x}(t) = Ax(t) + iBu(t), \quad x(0) = x_0 \quad (12)$$

where the field-free evolution is described by a Hermitian matrix $A \in C^{m \times n}$ with 0 as a simple eigenvalue and where the interaction with a low-dimensional control, $u(t) \in R^m, m \ll n$, is given by the input matrix $B \in R^{n \times m}$. However, for quantum systems governed by the Hamiltonian given in (1), driven by external control field(s), $u_k(t) \equiv F_k(t)$, we are dealing with a bi-linear input equation

$$\dot{x}(t) = \left(A + i \sum_{k=1}^m u_k(t) N_k \right) x(t), \quad x(0) = x_0 \quad (13)$$

where now the control term depends on both the field components, $u_k(t)$, and the state vector, $x(t)$. While identification with the TDSE (8) is straightforward, re-writing the LvNE (10) into this form is based on suitable vectorization of the density matrix $\rho(t)$. For the corresponding matrix representations of the commutators and anticommutators, see appendix A of Ref. [38].

Next, we introduce an equilibrium state x_e defined as $Ax_e = 0$. In the case of the TDSE (8), this is typically the ground state (after shifting its energy to zero), whereas in case of the LvNE (10) this is the thermal equilibrium defined by temperature Θ in the construction of the Lindblad operators obeying microscopic reversibility (B2), see App. B. Upon shifting the state vectors $x(t) \rightarrow x(t) - x_e$ and setting $b_k \equiv N_k x_e$, the following equation of motion is retrieved

$$\dot{x}(t) = \left(A + i \sum_{k=1}^m u_k(t) N_k \right) x(t) + i \sum_{k=1}^m u_k(t) b_k, \quad x(0) = x_0 - x_e \quad (14)$$

which is implemented in the WAVEPACKET functions `qm_control` and `qm_optimal` described in Secs. VI and VII. The shifted equation is now inhomogeneous and therefore more complicated. However, for an equilibrium initial condition, we have $x(0) = 0$ which is required for dimension reduction, see Secs. VIII-X.

C. Output equations

In LTI system theory [50], the output equation defines observables $y(t) \in R^p, p \ll n$, in terms of an output matrix $C \in R^{p \times n}$

$$y(t) = Cx(t) \quad (15)$$

For open quantum systems described by the LvNE (10), we rewrite this in terms of components

$$y_q(t) = c_q^\dagger x(t) + c_q^\dagger x_e, \quad q = 1, \dots, p \quad (16)$$

where we have again shifted the state vectors $x(t) \rightarrow x(t) - x_e$ and where the observables are represented by vectors $c_q \in R^n$. They are obtained by suitable mapping of the trace formula (11), see again appendix A of Ref. [38].

For closed quantum systems described by the TDSE (8), one has to consider quadratic output equations

$$y_q(t) = x^\dagger(t) D_q x(t) + 2\Re(x_e^\dagger D_q x(t)) + x_e^\dagger D_q x_e, \quad q = 1, \dots, p \quad (17)$$

where every observable is represented by a Hermitian matrix $D_q \in R^{n \times n}$ obtained as a matrix representation of Eq. (9). Because the WAVEPACKET functions `qm_control` and `qm_optimal` offer the choice of linear (16) or quadratic (17) output, those functions can be used both for LvNE and TDSE control problems.

D. Usage notes

By default, the WAVEPACKET function `qm_abncd` reads data from unformatted MATLAB data file `tise.mat` provided by function `qm_matrix`, see Sec. IV above. After having set up the A, B, N, C , or D matrices, the WAVEPACKET function `qm_abncd` writes them to unformatted data files named `tdse.mat` or `lvne.mat` for simulations of closed or open quantum systems, respectively. Alternatively, data files containing A, B, N, C , or D matrices can also come from other sources. As an example we mention here semi-discretized Fokker-Planck equations, which can also be written in the form of Eqs. (13) or (14), see our work in Refs. [37, 40].

E. Example: Morse oscillator with dissipation

As an example, let us consider the Morse oscillator from the previous sections, now interacting with a thermal bath through the linear SBC model of Eq. (2). This can be realized by adding the following lines to the WAVEPACKET initialization function `qm_init` before running `qm_abncd('lvne')`

```

global control
control.lvne.temperature = 0;
control.lvne.order = 'df';
control.relax.rate = 2*atomic.t.ps;
control.relax.lower = 0;
control.relax.upper = 1;
control.relax.model = 'fermi';

```

The second line is used to set the temperature, here $\Theta = 0$, while the third line specifies the ordering of the density matrix elements. Here 'df' stands for "diagonals first" which is the recommended option, see again App. A of Ref. [38]. The next three lines serve to set the relaxation rate, here $\Gamma_{0\leftarrow 1} = 2 \text{ ps}^{-1}$, and the last line is intended to select the relaxation model (based on Fermi's golden rule) to calculate all other rates, as described in App. B.

Here, the resulting matrices A and N are of dimension 484×484 with a density of 0.3 % and 8.8 %, respectively. Hence, our codes are exploiting the MATLAB support for sparse matrices. As an example we show the spectrum of matrix A in Fig. 2. The imaginary parts of the eigenvalues give the Bohr frequencies for transitions between bound states of the Morse oscillator under investigation whereas the real parts are essentially determined by the total dephasing rates [38]. Note that more negative values of the real parts indicate faster decay. We observe that the dephasing is fastest for transitions between states which are energetically near-by, see Eq. (B3) and Ref. [51].

Furthermore, the function `qm_abncd` also serves to specify the initial quantum state $|\Psi_0\rangle$ or the initial density matrix $\hat{\rho}_0$ for solving the TDSE (8) or the LvNE (10), respectively. Here we select a pure $v = 5$ state which can be prepared, e. g., employing an intense 1 ps infrared laser pulse, see Ref. [43] as well as Sec. 4.5 of Part I.

```

control.initial.choice = 'pure';
control.initial.pure = 5;

```

Other possible keywords for initializing an LvNE simulation of open quantum systems are 'cat' or 'mixed' for a coherent ("Schrödinger cat") or incoherent superposition of two states, respectively, or 'thermal' for a Boltzmann distribution.

Finally, in function `qm_abncd` there is also a choice of which of the observables defined in `qm_matrix` should be used as control targets. For example, setting the following

```
control.observe.targets = 1:7;
```

serves to specify that all 7 observables (of type 'prj') defined near the end of Sec. IV B are to be used for the output equations.

VI. QM_CONTROL

A. Solving the bi-linear control system

After the TDSE (8) or the LvNE (10) describing the dynamics of a closed or open quantum system, respectively, have been cast into the system matrices A, B, N, C or D by virtue of the WAVEPACKET function `qm_abncd`, the function `qm_control` can be used to solve the corresponding bi-linear control problem. It consists of the input equation (14) and output equations (16) or (17), see Secs. V B and V C. Normally, function `qm_control` solves the input equation by means of one of MATLAB's built-in ODE solvers. By default, it uses `ode45`, a versatile medium order method for systems of non-stiff ODEs; other choices are also possible. In doing so, each of the main time steps specified by the user, see Sec. 4.4 of Part I, is adaptively divided into sub-steps using a Dormand-Prince scheme, with the number of sub-steps depending on the relative tolerance which can be specified by the user. In addition to writing all relevant output to data files, function `qm_control` also generates graphics, in particular showing the control field $u(t)$, the state vector $x(t)$, and the observable output $y(t)$.

B. Example: Vibrational control and relaxation in a Morse oscillator

Here we continue with our discussion of the Morse oscillator of Ref. [43] with dissipation as detailed in Sec. V E, again using the Lindblad model of Eq. (B3) with relaxation rate $\Gamma_{0\leftarrow 1} = 2 \text{ ps}^{-1}$. In order to simulate field-free relaxation dynamics occurring during 1 ps, divided into 100 main time steps, the following lines are added to `qm_init`

```
global time
time.main.delta = 10/atomic.t.fs;
time.main.start = 0;
time.main.stop = 100;
```

```
control.solvers.handle2 = @ode45;
control.solvers.reltol = 1e-6;
```

where the last two lines serve to select the function handle for MATLAB's Dormand-Prince `ode45` integrator and to specify the relative tolerance of the numerical integration. Fig. 3 shows the vibrational relaxation dynamics for the chosen Morse oscillator. Assuming only the $v = 5$ state to be initially prepared, the system relaxes in a ladder-wise fashion until the ground state population takes over around $t = 824$ fs.

Also the competition of vibrational excitation and relaxation can be studied using the function `qm_control`. Fig. 4 shows the results of a 2 ps simulation using the same relaxation rates as before but employing a strong, intense, infrared laser pulse during the first picosecond, see Sec. 4.5 of Part I. As explained there, the pulse is designed to transfer nearly 100% of the population from the $v = 0$ to the $v = 5$ state for the case of a closed quantum system ($\Gamma \rightarrow 0$). Here, however, the coupling to the environment reduces this population transfer down to 13%. At the same time, the vibrational state selectivity is completely lost as can be seen from the approximately equal populations of $1 \leq v \leq 5$ states around $t = 726$ fs.

VII. QM_OPTIMAL

A. Quantum optimal control theory

This section deals with the application of optimal control theory (OCT) to a bi-linear control system consisting of input equation (14) and output equations (16) or (17), as described in Secs. V and VI. In the most frequently used version of OCT in quantum dynamics, the final time T is fixed and the task is to find field(s) $u_k(t)$ that drive the system from its initial state $x(t=0) = x_0$ to a final state $x(t=T)$ such that a specified observable κ is maximized at final time. This is equivalent to maximizing one of the three forms of linear or quadratic target functionals implemented in `WAVEPACKET`

$$\begin{aligned} J_{1a}[u, x] &= x^\dagger(T) D_\kappa x(T) + 2\Re(x_e^\dagger D_\kappa x(T)) \\ J_{1b}[u, x] &= \Re(c_\kappa^\dagger x(T)) \\ J_{1c}[u, x] &= |c_\kappa^\dagger x(T)|^2 \end{aligned} \tag{18}$$

where constant terms $c_\kappa^\dagger x_e$ or $x_e^\dagger D_\kappa x_e$ resulting from the equilibrium shift of the input equation (14) have been omitted. Functionals J_{1a} and J_{1b} are for optimization of the expectation value of a (positive definite) operator in simulations of a closed (TDSE, [31]) or open (LvNE, [32]) quantum system, respectively, see also Eqs. (17) and (16). Note again that in the latter case the vector c_κ is obtained by suitable vectorization of matrix D_κ representing the target observable, see Sec. V C. The third functional J_{1c} is for the special case of obtaining populations from overlaps in TDSE simulations, see our remarks in Sec. IV and Ref. [30]. Even though we assume here the optimization of a single target observable only, generalization to multi-target OCT is straight-forward [7, 8].

In addition to maximizing the target functional, it is often of importance to keep the energy associated with the control field (e. g., the laser fluence) bounded. Formally, this requirement can be expressed in terms of a cost functional

$$J_2[u] = \sum_k \alpha_k \int_0^T dt u_k^2(t)/s_k(t) \quad (19)$$

which is to be minimized. The penalty factors $\alpha_k > 0$ balance the importance of the cost functional against that of the target functional and/or balance the importance among the various field components k . The shape functions $s_k(t)$ can be used to enforce certain shape(s) of the field envelope, e. g., to model the typical switch on/off behavior of pulsed control fields [52].

Finally, the requirement of physically correct evolution of the system can be written as another functional to be minimized

$$J_3[u, x, z] = 2\Re \int_0^T dt z^\dagger(t)(\partial_t - \hat{L}(t))(x(t) + x_e) \quad (20)$$

where a Lagrange multiplier $z(t)$ has been introduced here to enforce that the state vector $x(t)$ satisfies its evolution equation $\partial_t x(t) = \hat{L}(t)(x(t) + x_e)$ and where the operator \hat{L} stands for the right-hand side of Eq. (14). Since we require the evolution to be fulfilled by the Hermitian conjugate of the evolution as well, we consider here the real part of the functional. We note that the inclusion of further constraints is also possible, see for example Refs. [34, 35] which is, however, not yet implemented in WAVEPACKET.

The necessary conditions for the combined functional $J \equiv J_1 - J_2 - J_3$ to become extremal can be seen directly from Pontryagin's principle. For a detailed derivation by means of standard variational calculus we recommend the tutorial by Werschnik and Gross [35]. The three conditions are as follows:

1. The state vector $x(t)$ is propagated forward via the input equation (14)

$$\dot{x}(t) = \hat{L}x(t) = \left(A + i \sum_{k=1}^m u_k(t) N_k \right) (x(t) + x_e) \quad (21)$$

starting from the initial condition $x(t=0) = x_0$.

2. The Lagrange multiplier $z(t)$ is propagated backward via the adjoint equation

$$\dot{z}(t) = -\hat{L}^\dagger z(t) = \left(-A^\dagger + i \sum_{k=1}^m u_k(t) N_k^\dagger \right) z(t) \quad (22)$$

starting from the final condition $z(t=T) = D_\kappa x(T) + D_\kappa x_e$ when optimizing J_{1a} or from $p(t=T) = c_\kappa$ when optimizing J_{1b} or J_{1c} . For the special case of anti-Hermitian evolution \hat{L} (e. g. anti-Hermitian A and real symmetric N for closed quantum systems, TDSE) we have the same propagators for state vector $x(t)$ and the Lagrange multiplier $z(t)$.

3. The optimized control field for control targets of the form J_{1a} or J_{1b} , see Eq. (18), is given by

$$u_k(t) = -\frac{s_k(t)}{\alpha_k} \Im \left(z^\dagger(t) N_k (x(t) + x_e) \right) \quad (23)$$

Optimizing targets of type J_{1c} in Eq. (18), as proposed in Ref. [30] for the TDSE case and in Ref. [32] for the LvNE case, offers the advantage that the initial condition of the backward propagations becomes independent of previous (forward) propagations. However, in such cases there has to be an additional factor $(x(t) + x_e)^\dagger z(t)$ inside the imaginary part of Eq. (23) for the optimal control field. While in theory this factor is independent of time t , in the practice of numerical optimization this is often not the case. Some authors, cf., Ref. [35] evaluate this at every time t , others recommend choosing $t = 0$ for forward and $t = T$ for backward propagations, see e. g. the Appendix of Ref. [30]. In WAVEPACKET there is a choice between all three options.

Within the WAVEPACKET function `qm_optimal` there is a choice of different Runge–Kutta and related integrators to solve the first order ODEs giving the evolution (21) of state vector $x(t)$ and the evolution (22) of Lagrange multiplier $z(t)$ which are coupled through the optimal control field(s) $u_k(t)$. Typically, these integrators also require knowledge about the value of the field at different times within each of the discretization interval, e. g. $u(t+\Delta t/2)$

for evaluating the midpoint rule. As suggested in Refs. [30, 31], the time dependence of $u_k(t)$ can be approximated by a linearization. The necessary derivative of the field are readily obtained by inserting (21) and (22) into the derivative of (23)

$$\dot{u}_k(t) = -\frac{s_k(t)}{\alpha_k} \Im \left(z^\dagger(t) (N_k A - A N_k) (x(t) + x_e) \right) \quad (24)$$

Note that within the WAVEPACKET function `qm_optimal` only integrators with fixed substep size can be used; for example several Runge-Kutta type methods have been implemented.

B. Iterative schemes

The system of the three coupled control equations (21)–(23) is routinely solved by the rapid monotonically convergent iterative algorithms of Refs. [30–35]. These schemes are initialized by propagating the state vector $x(t)$ forward in time using Eq. (21). In doing so, the initially (“guess”) field is typically assumed to be constant in time, and its amplitude has to be chosen strong enough to induce some notable dynamics. Then each step (for $n \geq 1$) of the iteration consists of the following:

- Propagate the Lagrange multiplier $z(t)$ backward in time using Eq. (22) with the field

$$\bar{u}_k^{(n)}(t) = (1 - \eta) u_k^{(n-1)}(t) - \eta \frac{s_k(t)}{\alpha_k} \Im \left((z^{(n)}(t))^\dagger N_k (x^{(n-1)}(t) + x_e) \right) \quad (25)$$

- Propagate the state vector $x(t)$ forward in time using Eq. (21) with the field

$$u_k^{(n)}(t) = (1 - \zeta) \bar{u}_k^{(n)}(t) - \zeta \frac{s_k(t)}{\alpha_k} \Im \left((z^{(n)}(t))^\dagger N_k (x^{(n)}(t) + x_e) \right) \quad (26)$$

This is repeated until the change in the total functional $J^{(n)} - J^{(n-1)}$ falls below a user-specified threshold. The two coefficients η and ζ describe the mixing of fields obtained for the recent and the previous iteration steps. In Refs. [33, 53] it is shown that monotonic convergence is found if η and ζ are between 0 and 2. Note that for the special case of $\eta = \zeta = 1$, we retrieve the scheme introduced by Zhu, Botina, and Rabitz [30, 31], while for $\eta = 0$ and $\zeta = 1$ the Krotov method is retrieved [54]. For a specific LvNE example system, the convergence behavior for different values of η and ζ is investigated numerically in Ref. [34], showing large variations in the number of iteration steps required to achieve a specified tolerance.

The above algorithms are frequently used in the molecular physics/chemistry community where molecular states are typically manipulated by pulsed lasers. However, in the physics community, often dealing with the manipulation of spin systems by NMR, there appears to be a preference for gradient ascent pulse engineering (GRAPE) algorithms [16, 55]. Those will be included in future versions of WAVEPACKET, with the aim of allowing for direct numeric comparisons for our default demonstration examples.

Finally, it is noted that the function `qm_optimal` also generates graphics 'on the fly', i. e., the control field $u(t)$, the state vector $x(t)$, and the observable output $y(t)$ can be viewed during the repeated forward and backward propagation. The animated graphics is also stored as an MPG file for later use in presentations etc.

C. Example: Optimized population transfer in a Morse oscillator

We return to the example of the Morse oscillator used throughout the previous sections. Here we consider the fundamental excitation from the ground state $|0\rangle$ to the first excited state $|1\rangle$. Even though this is a rather simple task, it shall serve here to illustrate the use of WAVEPACKET for such a quantum optimal control simulation. The following keywords have to be set within `qm_init.m` before running `qm_optimal`

```
control.optimal.terminal = 2;
control.optimal.max_iter = 50;
control.optimal.tolerance = 1e-10;
control.optimal.alpha = 1.0;
control.optimal.eta = 1.0;
control.optimal.zeta = 1.0;
```

The first line specifies the control target (to be evaluated at terminal time), here the second of the seven different populations specified at the end of Sec. IV B, i. e. the population of the first vibrationally excited state of the Morse oscillator. The following two lines serve to set the termination criteria for the iterative procedure, either after 50 iterations or after the change in the overall control functional falls below the specified tolerance. The remaining lines specify the "penalty" factor α as well as the prefactors η and ζ , see Eqs. (25,26).

The initial guess for the control field is set in the same way as for the WAVEPACKET functions `qm_propa` and `qm_control`; for an example see Sec. 4.5 in Part I. Note that the

shape of the envelope, here a \sin^2 -shaped half wave of 1 ps duration, serves also as a shape function $s(t)$ during the simulations, see Eq. (23).

Results of a TDSE simulation of a closed quantum system, where the populations are obtained from projection operators using target functional J_{1a} are shown in the left column of Fig. 5. We observe that the population of the target functional (population of $|1\rangle$) rises slowly but continuously during the iterations. After 10 cycles it reaches 71 %, after 100 cycles more than 93 %. At the same time, also the cost functional (fluence of the laser pulse) is rising. However, since the former one rises faster than the latter one, the overall control functional is still rising monotonically; for a formal proof, see Ref. [31]. The resulting pulse is essentially monochromatic; due to the prescribed \sin^2 shape, the envelope has a smooth switch-on and switch-off, and it is approximately symmetric within the 1 ps time window.

The central column of Fig. 5 shows the same but for an LvNE simulation of an open quantum system, here for $\Gamma_{0\leftarrow 1} = 1.24 \text{ ps}^{-1}$. For the vectorized densities, a target functional of type J_{1b} is optimized. Even though the cost functional J_2 shows that the resulting pulses are more intense, the efficiency of populating the excited state $|1\rangle$ is much lower. Another major difference lies in the shape of the envelope of the resulting laser pulse. Here, the highest amplitude occurs only after approximately three quarters of the prescribed time window of 1 ps. Obviously, the optimization avoids creating excited state population too early because it would relax back to the ground state before the final time.

The right column of Fig. 5 shows again a TDSE simulation. In contrast to the results shown in the left column of that figure, now the populations are calculated from overlaps using a target functional of type J_{1c} , see Eq. (18) and also Sec. IV. Already after the first iteration, the population of the target state is already exceeding 99 %. During the following iteration steps, the total function J increases further because the cost functional J_2 is reduced substantially which is in accordance with results of Ref. [30].

VIII. QM_BALANCE

A. Model reduction and the \mathcal{H}_2 error

The central task in dimension reduction is to find lower-dimensional (reduced) systems which approximate the input-output behavior of a driven dynamical system, see Secs. V B

and VC, as closely as possible on any compact time interval $[0; T]$. In practice this means that the \mathcal{H}_2 error norm has to be made as small as possible. In order to calculate this error, consider the following error system [42]:

$$A_E = \begin{bmatrix} A & 0 \\ 0 & \hat{A} \end{bmatrix}, N_{k,E} = \begin{bmatrix} N_k & 0 \\ 0 & \hat{N}_k \end{bmatrix}, B_E = \begin{bmatrix} B \\ \hat{B} \end{bmatrix}, C_E = \begin{bmatrix} C & -\hat{C} \end{bmatrix} \quad (27)$$

where the matrices without and with hats stand for the original and the reduced system, respectively. Here, as well as in the following Secs. IX and X, we will restrict ourselves to the case of open quantum systems modeled in terms of an LvNE, because there model reduction is more important than for TDSE calculations.

Once the error system has been set up, a generalized Lyapunov equation

$$A_E W_E + W_E A_E^\dagger + \sum_{k=1}^m N_{k,E} W_E N_{k,E}^\dagger + B_E B_E^\dagger = 0 \quad (28)$$

has to be solved; for remarks how to solve such an equation, see below. The resulting Gramian W_E can be used to obtain the \mathcal{H}_2 error norm as follows

$$\mathcal{E}_{\mathcal{H}^2} = \left(C_E W_E C_E^\dagger \right) = \left(B_E^\dagger W_E B_E \right) \quad (29)$$

which is often used to quantify the error introduced by dimension reduction. For example, within WAVEPACKET it can be calculated in the auxiliary functions `qm_H2error` and `qm_BTversush2`. Note, however, that the derivation of the \mathcal{H}_2 norm is based on output components generated by a δ -like (impulse) input components [50]. Hence, it is often mandatory to also consider the time-dependence generated by specific inputs, see e. g. our work in Refs. [37, 38].

B. Generalized Lyapunov equations

The problem of dimension reduction is closely connected to the concepts of controllability and observability (which are dual to each other). They are characterized in terms of Gramian matrices W_C and W_O , respectively. Their direct calculation involves a Volterra series with multiply nested time integrals [38]. In practice, however, it is of advantage to obtain the Gramians as the symmetric, positive semi-definite solutions of generalized Lyapunov equations. For the case of a bilinear input equation (13) and a linear output equation

(16) they are given by [56, 57]

$$\begin{aligned} AW_C + W_C A^\dagger + \sum_{k=1}^m N_k W_C N_k^\dagger + BB^\dagger &= 0 \\ A^\dagger W_0 + W_0 A + \sum_{k=1}^m N_k^\dagger W_0 N_k + C^\dagger C &= 0 \end{aligned} \quad (30)$$

where matrices B and C comprise all vectors b_k and c_q , respectively, see Sec. V. Because direct methods for solving such equations have a numerical complexity of $\mathcal{O}(n^6)$, two alternative approaches are implemented in the WAVEPACKET function `qm_balance`. The first one is based on mapping the Gramian matrices onto vectors. Then the generalized Lyapunov equations can be understood as systems of coupled linear equations which can be solved, e. g., by means of the bi-conjugate gradient method available in the `bicg` function of MATLAB. It is advantageous to pre-condition the problem by the solution of the standard Lyapunov equation, i. e. for $N_k = 0$. Alternatively, the following iteration can be used [58, 59]

$$\begin{aligned} AX_0 + X_0 A^\dagger + BB^\dagger &= 0 \\ AX_j + X_j A^\dagger + \sum_{k=1}^m N_k X_{j-1} N_k^\dagger + BB^\dagger &= 0, j > 0 \end{aligned} \quad (31)$$

and similarly for the second (dual) equation for the observability Gramian. For r iteration steps this only requires $\mathcal{O}(rn^3)$ operations, because WAVEPACKET solves the standard Lyapunov equations in each step by the Bartels-Stewart algorithm implemented in function `lyap` provided with the control toolbox of MATLAB.

Convergence $X_j \rightarrow W_C$ is guaranteed if the eigenvalue of A with the largest (negative) real part is sufficiently separated from the imaginary axis [58]. For linear control systems (with $N_k = 0$) the Lyapunov equations can always be solved if matrix A is stable, i. e. having all its eigenvalues in the open left half of the complex number plane. Stability thus means that there are constants $\lambda, a > 0$ such that $\|\exp(At)\| \leq \lambda \exp(-at)$. For systems where this is not the case, e. g., for the LvNE (10) with Lindblad dissipation/dephasing, WAVEPACKET offers two numeric stabilization techniques, see App. C. For non-linear control systems, where the generalized Lyapunov equations (30) have to be solved, the controllability and observability Gramians exist only if

$$\frac{\lambda^2}{2a} \sum_{k=1}^m \|N_k\|^2 < 1 \quad (32)$$

where $\|\cdot\|$ is the matrix 2-norm induced by the Euclidean norm $|\cdot|$. This can be assured by a suitable scaling $u \rightarrow \xi u, N \rightarrow N/\xi, B \rightarrow B/\xi$ with real $\xi > 1$ which leaves the equations of motion invariant but not the Gramians. Hence, by increasing ξ , we can ensure solvability of (30). In our numeric WAVEPACKET experiments reported in Ref. [37], we observe a sensitive dependence on the value of this scaling factor. In some cases, good results are obtained only for large scaling factors. However, because this scaling drives the system toward its linear counterpart, the parameter ξ should not be chosen larger than necessary.

C. Balancing controllability and observability

In heuristic approaches to dimension reduction, states are often excluded because they are not reachable by external control fields (not *controllable*) or because they do not contribute to the specified control target (not *observable*). However, model order reduction can become more challenging when states that are observable are not controllable or vice versa. This is the motivation for the balancing transformation which strives at finding states which are controllable and observable at the same time. The idea of such a transformation rests on the transformation properties of a control system, applied to its controllability and observability Gramians [50]. Upon linear change of coordinates, the state vectors and system matrices transform according to

$$\begin{aligned}\tilde{x} &= Sx \\ \tilde{A} &= SAT \\ \tilde{N}_k &= SN_kT \\ \tilde{b}_k &= Sb_k \\ \tilde{C} &= CT\end{aligned}\tag{33}$$

where $T=S^{-1}$ is the inverse of S (for the case of square, invertible S) or the pseudoinverse of S with $STS = S$ and $TST = T$ (if S is singular or rectangular). This implies the following transformations for the controllability and observability Gramians

$$\begin{aligned}\tilde{W}_C &= SW_C S^\dagger \\ \tilde{W}_O &= T^\dagger W_O T \\ \tilde{W}_C \tilde{W}_O &= SW_C W_O T\end{aligned}\tag{34}$$

While the eigenvalues of the Gramians W_C and W_O are not invariant, those of the product of the Gramians are invariant under the similarity transformation.

The central idea of balancing is to find a coordinate transformation under which controllability and observability Gramians become equal and diagonal

$$\tilde{W}_C = \tilde{W}_O = \Sigma \quad (35)$$

where Σ is a diagonal matrix. Its elements $\sigma_i > 0$ are known as Hankel singular values (HSVs) of the system; they are the square roots of the product of the Gramians. Note that the transformation is a contragredient transformation which exists whenever W_C and W_O are symmetric and positive definite [60]. In the balanced representation, states that are least influenced by the input also have the least influence on the output and vice versa, see for an example Fig. 5 of our work in Ref. [37]. Within the `WAVEPACKET` function `qm_balance`, there is a choice of two different approaches to find the desired transformation. One is the "Square Root Balanced Truncation" (SRBT) algorithm [60, 61], the other is the "Minimal Realization and Model Reduction" (MRMR) algorithm [62].

D. Example code

Here we are giving a few examples how to set the most important keywords, typically within `qm_init`, before running `qm_balance` to carry out the balancing transformation.

```
reduce.balance.BN_scale = 6;
reduce.balance.method = 'iter';
reduce.balance.transform = 'srbt';
reduce.balance.A_stable = 'ssu';
reduce.balance.A_split = 1;
```

In the first line, the scaling factor ξ for upscaling the field $u(t)$ and downscaling the matrices B, N has been set to 6. The second line specifies the method of solving the generalized Lyapunov equations (30) which can be either `'iter'` for the iterative solver (31) or `'bicg'` for the bi-conjugate gradient method. In the third line, the SRBT balancing method has been chosen, see above. Furthermore, the stabilization of the A matrix is achieved by separating the stable from the unstable part (`'ssu'`), where in the case of LvNE dynamics there is only

one unstable component that has to be split off, see also App. C. Alternatively, a shift of the eigenvalues ('`evs`') of the A matrix can be invoked by the following statements

```
reduce.balance.A_stable = 'evs';
reduce.balance.A_shift = 1e-4;
```

with $\alpha = 10^{-4}$, see again App. C. Finally, it is noted that the WavePacket function `qm_balance` reads the original A, B, N, C matrices from an unformatted data file `lvne.dat` for simulations of open quantum systems, respectively. Upon transformation, the balanced $\tilde{A}, \tilde{B}, \tilde{N}, \tilde{C}$ matrices are written to a file named `lvne_b.mat`, see Fig. 1.

IX. QM_TRUNCATE

A. Decomposition of the balanced system

By its very construction, the balancing transformation implies that those states corresponding to large HSVs ($x_1 \in \mathbf{R}^d$) are more controllable and more observable than those states corresponding to small HSVs ($x_2 \in \mathbf{R}^{n-d}$). Then the matrix Σ can be written as $\Sigma = (\Sigma_1, \Sigma_2)$ where $\Sigma_1 \in \mathbf{R}^{d \times d}$ and $\Sigma_2 \in \mathbf{R}^{(n-d) \times (n-d)}$, according to the decomposition of the system states into relevant and irrelevant states [39, 40]. Using corresponding decompositions of A, b, N, C , one obtains the coupled equations of motion

$$\begin{aligned}\dot{\tilde{x}}_1 &= \tilde{A}_{11}\tilde{x}_1 + \tilde{A}_{12}\tilde{x}_2 + \sum_{k=1}^m \left(\tilde{N}_{k,11}\tilde{x}_1 + \tilde{N}_{k,12}\tilde{x}_2 + \tilde{b}_{k,1} \right) u_k \\ \dot{\tilde{x}}_2 &= \tilde{A}_{21}\tilde{x}_1 + \tilde{A}_{22}\tilde{x}_2 + \sum_{k=1}^m \left(\tilde{N}_{k,21}\tilde{x}_1 + \tilde{N}_{k,22}\tilde{x}_2 + \tilde{b}_{k,2} \right) u_k \\ y &= \tilde{C}_1\tilde{x}_1 + \tilde{C}_2\tilde{x}_2\end{aligned}\tag{36}$$

In the following, we explain the two approaches implemented in WAVEPACKET function `qm_truncate` to deal with the coupled sets of equations.

B. Simple truncation

The simplest approach to dimension reduction simply consists of a truncation of the less controllable and less observable states x_2

$$\begin{aligned}\dot{\tilde{x}}_1 &= \tilde{A}_{11}\tilde{x}_1 + \sum_{k=1}^m \left(\tilde{N}_{k,11}\tilde{x}_1 + \tilde{b}_{k,1} \right) u_k \\ y &= \tilde{C}_1\tilde{x}_1\end{aligned}\tag{37}$$

This can be justified as being the $\epsilon \rightarrow 0$ limit of (36) assuming $\Sigma_2 = \mathcal{O}(\epsilon)$ with $0 < \epsilon \ll 1$, see Ref. [37]. The truncated subsystem x_1 is balanced and stable, and - at least for the case of linear systems - an upper bound for the error of its transfer function is known [50].

C. Singular perturbation theory

Alternatively, an averaging principle based on singular perturbation theory can be used, in a similar spirit to the treatment of systems with slow and fast degrees of freedom (dof's) [39, 40]. Based on the analogy between large HSV-modes with slow dof's and low HSV-modes with fast dof's, we assume that the latter ones to have relaxed to their steady state, $\tilde{x}_2 \rightarrow -\tilde{A}_{22}^{-1}\tilde{A}_{21}\tilde{x}_1$ for the $t \rightarrow \infty$ limit. Then one can derive equations of motion for \tilde{x}_1 which look like (37) but with the following substitutions

$$\begin{aligned}\tilde{A}_{11} &\rightarrow \tilde{A}_{11} - \tilde{A}_{12}\tilde{A}_{22}^{-1}\tilde{A}_{21} \\ \tilde{N}_{k,11} &\rightarrow \tilde{N}_{k,11} - \tilde{N}_{k,12}\tilde{A}_{22}^{-1}\tilde{A}_{21} \\ \tilde{C}_1 &\rightarrow \tilde{C}_1 - \tilde{C}_2\tilde{A}_{22}^{-1}\tilde{A}_{21}\end{aligned}\tag{38}$$

Both the simple truncation and the averaging principle have been implemented in the recent version of the WAVEPACKET function `qm.truncate`. However, in a series of numeric test calculations no clear preference for either one has been found, i. e. the (moderate) additional effort of the singular perturbation method seems not to lead to more accurate reduced models than the simple truncation [37].

D. Example: Asymmetric double well

Here we will switch to the one-dimensional asymmetric double well system considered also in our previous work [37, 38]. In addition to six (five) stationary quantum states which

are essentially localized in the left (right) well, we also include the first ten delocalized eigenstates; higher states are neglected for simplicity. The 21 considered states lead to a density matrix with dimension $n = 441$ thus rendering model order reduction very useful, e. g., during refinements of fields in quantum optimal control simulations.

The effect of truncation on the time-dependence of observables for given control fields, as well as a comparison of spectra of full versus reduced A matrices has already been shown in Refs. [37, 38]. Here we want to present results of quantum optimal control simulations using the WAVEPACKET function `qm_optimal` in full versus reduced dimensionality. First, we define as observables the total populations of all states in the left (energetically lower) well, in the right well, and of delocalized states above the barrier. The target of the optimization is the second of these observables, to be reached after 100 units of time. The results after 15 optimization cycles can be seen in Fig. ??, where control fields and observables after optimization are shown. For $0 < t < 30$ the field quasi-resonantly drives the system up the ladder of the quantum states localized inside each of the wells which is not reflected by the rather coarse observables. At later times, the field drives the population to the delocalized states over the barrier. From there the population finds its way back to the localized states, preferentially those in the right well, probably due to a combination of stimulated emission and dissipation. Comparing the left and right half of Fig. ?? shows that the optimized field, as well as the induced population dynamics, in full dimensionality ($n = 441$) practically coincides with that for a reduced order model ($d = 170$), obtained by balanced truncation using the WAVEPACKET functions `qm_balance` and `qm_truncate`. Upon further dimension reduction ($d = 160$) the optimized field changes qualitatively, thus indicating a limit to dimension reduction for use in optimal control of this model system.

X. QM_H2MODEL

A. \mathcal{H}_2 -optimal model reduction

This approach to dimension reduction of bilinear control systems is based on the idea of finding an \mathcal{H}_2 -optimal system that approximates as closely as possible the transfer matrix of the original system, i. e. minimizing the \mathcal{H}_2 - error introduced in Eq. (29). The method is inspired by the Bilinear Iterative Rational Krylov Algorithm (BIRKA) [37, 42]. Building

on the idea of iterative correction, this algorithm aims at fulfilling the first-order necessary optimality conditions, stated in terms of matrix equations. This allows to construct the required projection subspaces as solutions to generalized Sylvester equations.

In practice, the algorithm works as follows. The original n -dimensional bilinear control system (A, B, N, C) is to be approximated by a d -dimensional reduced order model $(\hat{A}, \hat{B}, \hat{N}, \hat{C})$. Initially chosen by random, the matrices characterizing the reduced system are refined by the following iteration:

B. Generalized Sylvester equations

In each iteration step, two generalized Sylvester equations have to be solved

$$\begin{aligned} AX + X\hat{A}^\dagger + \sum_{k=1}^m N_k X \hat{N}_k^\dagger + B\hat{B}^\dagger &= 0 \\ A^\dagger Y + Y\hat{A} + \sum_{k=1}^m N_k^\dagger Y \hat{N}_k - C^\dagger \hat{C} &= 0 \end{aligned} \quad (39)$$

yielding (rectangular) matrices $X, Y \in \mathbf{C}^{n \times d}$. Note the formal similarity with the generalized Lyapunov equations (30) for the calculations of Gramians; however, there is a sign change in the $C^\dagger C$ term. Another difference to the generalized Lyapunov equations is that a direct solution of the generalized Sylvester equations requires "only" $\mathcal{O}(d^3 n^3)$ operations where d denotes the dimension of the reduced model. As for the case of generalized Lyapunov equations, two alternative approaches are available within the `WAVEPACKET` function `qm_H2model`. One possibility is to rewrite the generalized equations as a linear problem which can be solved, e. g., by the bi-conjugate gradient method where it is advantageous to use the solutions of the corresponding ordinary Sylvester equations for pre-conditioning. Alternatively, iterative methods [58, 59] can be used instead which requires the solution of a standard Sylvester equation in each step

$$\begin{aligned} AX_0 + X_0\hat{A}^\dagger + B\hat{B}^\dagger &= 0 \\ AX_j + X_j\hat{A}^\dagger + \sum_{k=1}^m N_k X_{j-1} \hat{N}_k^\dagger + B\hat{B}^\dagger &= 0, j > 0 \end{aligned} \quad (40)$$

and similarly for the second (dual) equation for Y . Note that the cost for the solution of a standard Sylvester equations is less than for a standard Lyapunov equations also because the former ones can be handled efficiently for sparse system matrices. Hence, a single

step of the BIRKA iteration is computationally less expensive than performing a balancing transformation. However, the effort for BIRKA obviously depends on the number of iteration steps required until the fixed point iteration is (numerically) converged. Based on the numerical examples studied in Ref. [37], we can not report significant differences between the methods.

C. Fixed point iteration

Once the generalized Sylvester equations have been solved, a QR-decomposition of matrices X, Y is performed

$$\begin{aligned} X &= VR \\ Y &= WZ \end{aligned} \tag{41}$$

where V, W are orthogonal matrices and R, Z are upper triangular matrices (not needed here). Then V, W are used to construct a refined system in the following way

$$\begin{aligned} \hat{A} &= SAV \\ \hat{N}_k &= SN_k V \\ \hat{B} &= SB \\ \hat{C} &= CV \end{aligned} \tag{42}$$

which corresponds to a Petrov-Galerkin projection of the original model with

$$S = (W^\dagger V)^{-1} W^\dagger \tag{43}$$

Then the refined system (42) is inserted into the generalized Sylvester equations (39) yielding new matrices V, W . This iteration is repeated until the change in the spectrum of the reduced order system matrix \hat{A} falls below a user prescribed tolerance.

D. Example code

Here we give examples for keywords to be used with the function `qm.H2model` for \mathcal{H}_2 -optimal model reduction

```

reduce.H2model.A_stable = 'ssu';
reduce.H2model.A_split = 1;
reduce.H2model.BN_scale = 3;
reduce.H2model.method = 'iter';
reduce.H2model.max_iter = 200;
reduce.H2model.conv_tol = 1e-6;

```

The first three lines concerning the stabilization of A -matrix (by splitting off one unstable component) and the scaling of u, B, N are in close analogy to the keywords used for the balancing transformation, see Sec. VIII D. The fourth line is to indicate the use of the iterative solver (40) for generalized Sylvester equations (39). The last two lines specify termination criteria for the BIRKA iteration process, i. e., the maximum number of iterations and a convergence tolerance. Finally, it is noted that the WavePacket function `qm.H2model` reads the original A, B, N, C matrices from an unformatted data file `lvne.dat` for simulations open quantum systems, respectively. Upon transformation, the reduced $\hat{A}, \hat{B}, \hat{N}, \hat{C}$ matrices are written to a file named `lvne.h.mat`, see also Fig. 1.

For numeric experiments concerning the accuracy and the computation effort of the \mathcal{H}_2 -optimal model reduction, we refer the reader to Refs. [37, 42]. We have also repeated the calculations presented in Sec. IX D for the asymmetric double well model. This time we have compared optimized fields obtained for driven population dynamics for the full-dimensional ($n = 441$) model versus an \mathcal{H}_2 -optimal model, with very similar results: We found excellent agreement for $d = 170$, but notable deviations for $d = 160$, see also Fig. ??.

XI. SUMMARY AND OUTLOOK

Complementary to Part I which described the PDE based solvers for Schrödinger equations together with the underlying discrete variable representations implemented in WAVEPACKET, the present Part II discusses the ODE based approach to quantum dynamics in that program package, which allows to treat Schrödinger and Liouville-von Neumann equations on an equal footing. While so far only Lindblad-Kossakowski models for dissipation and dephasing have been implemented, also Redfield or other approaches would be straight-forward to be include. This generalization of the WAVEPACKET codes has also allowed for a relatively easy implementation of the rapid monotonically convergent algorithms

for optimal control of closed and open quantum systems. It can be expected that more recent developments in this field, such as multi-target optimization, time-averaged targets and also non-linear models for the interaction between quantum systems and external fields will become available in future versions of our software package.

While most of the above aspects are also available in other packages such as MCTDH, TDDVR, QUTIP and/or QLIB, an advantage of WAVEPACKET is that it offers a coherent combination of all these features, sharing the MATLAB functions for features such as the definition of the Hamiltonian etc. Moreover, it is emphasized that the target systems for WAVEPACKET are low- to medium-dimensional (model) systems where computational requirements are not the dominant concern, but user-friendliness and on-the-fly graphics are. For example, the FFT-based representations typically allow for 3...5 dimensional propagations using `qm_propa` or 2...3 dimensional bound state calculations using `qm_bound` on a standard PC equipped with 8 GB of memory, see also Sec. 7 of Part I. Alternatively, for dynamical simulations in energy representation using `qm_control`, the present version of WAVEPACKET can typically handle thousands of quantum states. Even though these limits can be pushed forward – to some extent – by resorting to more powerful hardware, the present software certainly does not aim at competing with the MCTDH or TDDVR package with respect to high dimensionality. However, we stress the role of the model order reduction available since version 5.0 of WAVEPACKET. Three different approaches, i. e., balanced truncation, singular perturbation theory, and \mathcal{H}_2 -optimal model reduction, have been implemented. So far, none of them has been shown to be superior to the others in our numeric experiments, despite of the quite different nature of the approaches. It remains to be seen how these algorithms perform for different classes of quantum systems. We hope that the public release will help to spread these algorithms in the research community, and we are expecting feedback from the users which will be also instrumental for the further development.

Since the advent of versions 4.x and 5.x, the WAVEPACKET framework is developed in MATLAB. Despite of limitations in the availability in some academic institutions, we chose that programming environment because it offers several unique features. There are built-in functions for many frequently used tasks, in particular in the field of numeric linear algebra, including support for sparse matrices, thus allowing for fast code development. Note that MATLAB is rather intuitive to use, due to the close proximity between physical/mathematical

formulations and the program codes. Furthermore, it offers an easy extension of core functionality through function handles, thus making it easy to apply the MATLAB version of WAVEPACKET to different physical situations. Moreover, graphical output, partly in the form of animations, is readily available to the user, which is helpful to develop a more intuitive understanding quantum dynamics and quantum optimal control.

In this context it may also be of interest how the choice of MATLAB affects the performance of WAVEPACKET. To this end, we compared the MATLAB version (described in the present work) with the C++ version (currently under development). For both versions most of the computational time is spent in external libraries such as FFTW, BLAS, so that the result strongly depends on the respective implementation of these libraries. Despite of the obvious limitations, we did a crude comparison between the Matlab and the C++ version. Contrary to common belief, our preliminary results show that the performance of the two versions is similar. Typically simulations with the MATLAB version of `qm_propa` using an FFT-based DVR/FBR schemes with 32 points in each dimensions take 41 (3D), 244 (4D), or 10600 (5D) seconds, for 2000 steps (Strang splitting) on a PC with Intel Xeon CPU (E3-1241 v3 @ 3.5 GHz). Finally, it is mentioned that due to the extensive use of advanced MATLAB features (cell arrays, structures, occasionally also classes), the WAVEPACKET software does not operate correctly under Gnu Octave.

For the next main version of WAVEPACKET it is planned to go beyond purely quantum-mechanical propagations by also offering functions for classical [63] and mixed quantum-classical dynamics [64, 65], including surface hopping algorithms [64, 66]. Since these generalizations are difficult to be implemented in a completely procedural way, the further development of the MATLAB version of WAVEPACKET will be directed toward object-oriented approaches. Note that first steps have already been implemented for the realizations of the DVR/FBR techniques described in Part I. At the same time, the above-mentioned C++ version aims at a rewrite of the WAVEPACKET codes in a completely object-oriented manner. However, as long as that project is still in an early stage, the MATLAB codes presented here will remain the main working version of WAVEPACKET for the next few years.

Since 2008, the development of the free and open-source WAVEPACKET is hosted at SOURCEFORGE, with the version described in this work being 5.3.0. In addition to an SVN repository providing a central location to manage the distributed development of our software package, there is also a large number of Wiki pages containing complete descriptions

of all the MATLAB functions, classes, and variables, serving as a reference to users. Further information about the physical and numerical background is also available on the Wiki pages of the WAVEPACKET main project, along with a large number of worked out demonstration examples, complete with input and output data files, often including animated graphics as MP4 files. These examples can also be understood as a tutorial, not only including all examples presented in Parts I and II of this work, but also demonstrating the use of our software package for model systems beyond one dimension, both for single and coupled Schrödinger equations.

Acknowledgments

This work has been supported by the Einstein Center for Mathematics Berlin (ECMath) through projects SE 11 and SE 20. Boris Schäfer-Bung (formerly at FU Berlin) and Tobias Breiten (U of Graz, Austria) are acknowledged for setting up initial versions of the MATLAB codes for dimension reduction. Finally, we are grateful to Ulf Lorenz (formerly at U Potsdam) for his valuable help with all kind of questions around the WAVEPACKET software package.

Appendix A: Compatibility issues

With the introduction of versions 5.3.0 a few minor backward incompatibilities have arisen. In particular there are a few changes in the initialization (normally provided through self-written Matlab function `qm_init.m`) with respect to version 5.2.3 described in Part I. These changes have become necessary because we decided to have (almost) all variables as MATLAB structures with three hierarchical levels, see Tab. I. Moreover, the class definitions for DVR/FBR grids and (associated) kinetic operators have been arranged into package folders, in order to be organized similarly to potentials, dipoles, etc. Hence, in the respective notations, underscores have to be replaced by dots, e. g. `grid_fft` has to be replaced by `grid.fft`. For more details about these syntax changes, the reader is referred to the news section in the Wiki pages of the MATLAB version of WAVEPACKET.

until V5.2.3	since V5.3.0
hamilt.pot.params.xyz	hamilt.pot.xyz
hamilt.dip.params.xyz	hamilt.dip.xyz
hamilt.nip.params.xyz	hamilt.nip.xyz
time.propa.params.xyz	time.propa.xyz
psi.init.dof{1}.xyz	psi.dof{1}.xyz

TABLE I: Change of fieldnames between different WavePacket versions where **xyz** stands for various possible field names

Appendix B: Dissipation and dephasing models

Within the WAVEPACKET software package, population relaxation (dissipation) and associated dephasing are described by Eq. (10) using Lindblad operators

$$\hat{L}_\ell = \hat{L}_{ij} = \sqrt{\Gamma_{i \leftarrow j}} |i\rangle \langle j| \quad (\text{B1})$$

where the summation extends over all possible channels $\ell = (i \leftarrow j)$. With the (phenomenological) rate constants given as inverse times $\Gamma_{i \leftarrow j} = 1/T_{i \leftarrow j}$ the Lindblad evolution is trace-preserving, i.e. the sum of populations remains constant, and completely positive, i. e., also the individual populations remain positive. Typically, the upward rates are calculated from the downward ones using the principle of detailed balance

$$\Gamma_{j \leftarrow i} = \exp \left(-\frac{E_j - E_i}{k_B \Theta} \right) \Gamma_{i \leftarrow j}, \quad j > i \quad (\text{B2})$$

which ensures that the densities approach the Boltzmann distribution for temperature Θ in the limit of infinitely long times.

Specific models for the rate constants defined in Eq. (B1) require - in principle - a microscopic knowledge of the system-bath coupling operator. Since this information is usually not available, simplifying assumptions have to be made. Two such models are currently available within the WavePacket function `qm.abncd`. The first one builds on the assumption that the system-bath coupling Hamiltonian is linear in the bath modes, see Eq. (2). Using Fermi's golden rule for the weak coupling limit, and assuming equal masses and frequencies of the bath modes, it can be shown that the downward (population) relaxation rates fulfill

the following relation (with $\omega_{ji} \equiv E_j - E_i$)

$$\Gamma_{i \leftarrow j} \propto \frac{\chi_{ji}^2}{\omega_{ji}} \frac{1}{\exp \frac{\omega_{ji}}{k_B T} - 1}, \quad j > i \quad (\text{B3})$$

see e. g. Ref. [51] for an application to molecular vibrations. Another frequently used model is based on scaled Einstein coefficients for spontaneous emission

$$\Gamma_{i \leftarrow j} \propto \mu_{ji}^2 \omega_{ji}^3, \quad j > i \quad (\text{B4})$$

see Ref. [67] for an application to molecular electronic dynamics. Together with the principle of detailed balance (B2), these two models only require the specification of one relaxation rate (typically $\Gamma_{0 \leftarrow 1}$) to determine all rates of a Lindblad model (10). As an alternative to these scaling relations, WAVEPACKET also offers the possibility to assume constant relaxation rates or to read pre-computed rates from input data files.

Within the WAVEPACKET software package, a frequently used model for pure dephasing can be described within the Lindblad model of Eq. (10) with operators

$$\hat{L}_\ell = \sqrt{2\kappa} \sum_\ell |\ell\rangle E_\ell \langle \ell| = \sqrt{2\kappa} \hat{H}_0 \quad (\text{B5})$$

where $\kappa > 0$ is a scaling factor. This leads to a quadratic energy gap dependence for the dephasing rate

$$\gamma_{ij}^* = \kappa \omega_{ij}^2 \quad (\text{B6})$$

see, e. g., Ref. [68] for an application on vibrational dephasing rates for molecules interacting with a bath. Alternatively, WAVEPACKET also offers the possibility to assume constant dephasing rates or to read those rates from input data files.

Appendix C: Stabilizing the A matrix

In stability theory, a stable system approaches a fixed point (an equilibrium) in the long time limit, and nearby points converge to it at an exponential rate. In the input equations (12,13) given in Sec. V B, assuming vanishing fields $u(t) = 0$, this requires that the spectrum of the system matrix A should be in the left half of the complex number plane (negative real part). Such matrices are also referred to as Hurwitz stable matrices.

However, for open quantum system dynamics we use the LvNE (10) with Lindblad superoperators describing relaxation to the thermal equilibrium x_e . Hence, matrix A has a

simple eigenvalue zero. In such cases, the A matrix can be stabilized by one of the following two techniques:

- The diagonal values of matrix A can be shifted by a small negative amount, $A \rightarrow A - \alpha I$, where $\alpha > 0$ is a real-valued shift parameter. Solutions of ODEs always contain a term of the form $\exp(At)$, hence this shift introduces a damping of the form $\exp(-\alpha t)$. In optimal control theory this is referred to as "discounting a functional", i.e., the further future is not taken quite as important as the closer future. This damping drives the system towards $x = 0$, i.e., to the equilibrium state, even for the case of closed quantum system dynamics described by TDSE, where this procedure may violate norm conservation.
- The unstable part of A can be separated by transforming the matrices A, N_k, C and the vectors $b_k, x(t)$ into the eigenbasis of A . If we order the eigenvalues by the absolute value of their real parts, we can directly separate the unstable part $x_1 \in C^M$ from the stable part $x_2 \in C^{n \times (n-M)}$. Since a straightforward implementation will – in general – destroy the sparsity pattern of the matrices involved, we suggest to use a particular technique for sparsity preserving projections, see Chap. 5.2 of Ref. [37]. Note that in the case of open quantum system dynamics described by LvNE (10) with Lindblad superoperators it is sufficient to choose $M = 1$, i.e. there is only one unstable component (eigenvalue zero) to be removed.

-
- [1] V. May and O. Kühn, *Charge and Energy Transfer Dynamics in Molecular Systems* (Wiley, Berlin, 2000).
- [2] W. P. Schleich, *Quantum Optics in Phase Space* (Wiley–VCH, Berlin, 2001).
- [3] D. Tannor, *Introduction to Quantum Mechanics. A Time-Dependent Perspective* (University Science Books, Sausalito, 2004).
- [4] F. Großmann, *Theoretical Femtosecond Physics* (Springer, Berlin Heidelberg, 2008).
- [5] A. H. Zewail, *The Journal of Physical Chemistry A* **104**, 5660 (2000).
- [6] V. Sundström, *Annual Review of Physical Chemistry* **59**, 53 (2008).
- [7] R. de Vivie-Riedle and U. Troppmann, *Chemical Reviews* **107**, 5082 (2007).

- [8] J. Zhu, S. Kais, Q. Wei, D. Herschbach, and B. Friedrich, *The Journal of Chemical Physics* **138**, 024104 (2013).
- [9] S. Kais, ed., *Quantum Information and Computation for Chemistry* (2014).
- [10] S. J. Glaser, U. Boscain, T. Calarco, C. P. Koch, W. Köckenberger, R. Kosloff, I. Kuprov, B. Luy, S. Schirmer, T. Schulte-Herbrüggen, et al., *The European Physical Journal D* **69**, 279 (2015).
- [11] M. H. Beck, A. Jäckle, G. A. Worth, and H.-D. Meyer, *Physics Reports* **324**, 1 (2000).
- [12] B. A. Khan, S. Sardar, P. Sarkar, and S. Adhikari, *The Journal of Physical Chemistry A* **118**, 11451 (2014).
- [13] J. R. Johansson, P. D. Nation, and F. Nori, *Computer Physics Communications* **183**, 1760 (2012).
- [14] J. R. Johansson, P. D. Nation, and F. Nori, *Computer Physics Communications* **184**, 1234 (2013).
- [15] C. B. Mendl, *Computer Physics Communications* **182**, 1327 (2011).
- [16] S. Machnes, U. Sander, S. J. Glaser, P. D. Fouqui, A. Gruslys, and S. Schirmer, *Physical Review A* **84**, 022305 (2011).
- [17] B. Schmidt and U. Lorenz, *Computer Physics Communications* **213**, 223 (2017).
- [18] J. C. Light, I. P. Hamilton, and J. V. Lill, *The Journal of Chemical Physics* **82**, 1400 (1985).
- [19] J. C. Light and T. Carrington, *Advances in Chemical Physics* **114**, 263 (2000).
- [20] C. Leforestier, R. Bisseling, C. Cerjan, M. Feit, R. Friesner, A. Guldberg, A. Hammerich, G. Jolicard, W. Karrlein, H.-D. Meyer, et al., *Journal of Computational Physics* **94**, 59 (1991).
- [21] M. Baer, *Beyond Born–Oppenheimer* (Wiley-VCH, Hoboken, New Jersey, 2006).
- [22] W. Domcke, D. R. Yarkony, and H. Köppel, eds., *Conical Intersections. Electronic Structure, Dynamics and Spectroscopy*, vol. 15 of *Advanced Series in Physical Chemistry* (World Scientific, Singapore, 2004).
- [23] U. Weiss, *Quantum Dissipative Systems* (World Scientific, Singapore, 1999).
- [24] H.-P. Breuer and F. Petruccione, *The Theory of Open Quantum Systems* (Oxford University Press, 2002).
- [25] A. Kossakowski, *Reports on Mathematical Physics* **3**, 247 (1972).
- [26] G. Lindblad, *Communications in Mathematical Physics* **48**, 119 (1976).
- [27] R. Judson and H. A. Rabitz, *Physical Review Letters* **68**, 1500 (1992).

- [28] H. A. Rabitz, R. de Vivie-Riedle, M. Motzkus, and K. Kompa, *Science* **288**, 824 (2000).
- [29] H. A. Rabitz, *Science* **299**, 525 (2003).
- [30] W. Zhu, J. Botina, and H. A. Rabitz, *The Journal of Chemical Physics* **108**, 1953 (1998).
- [31] W. Zhu and H. A. Rabitz, *Journal of Chemical Physics* **109**, 385 (1998).
- [32] Y. Ohtsuki, W. Zhu, and H. A. Rabitz, *The Journal of Chemical Physics* **110**, 9825 (1999).
- [33] Y. Maday and G. Turinici, *The Journal of Chemical Physics* **118**, 8191 (2003).
- [34] Y. Ohtsuki, G. Turinici, and H. A. Rabitz, *The Journal of Chemical Physics* **120**, 5509 (2004).
- [35] J. Werschnik and E. K. U. Gross, *Journal of Physics B: Atomic and Molecular Physics* **40**, R175 (2007).
- [36] C. Hartmann, J. C. Latorre, W. Zhang, and G. A. Pavliotis, *Journal of Computational Dynamics* **1**, 279 (2014).
- [37] P. Benner, T. Breiten, C. Hartmann, and B. Schmidt, *SIAM Journal on Applied Dynamical Systems (SIADS)*, submitted. arXiv:1706.09882 (2017).
- [38] B. Schäfer-Bung, C. Hartmann, B. Schmidt, and C. Schütte, *The Journal of Chemical Physics* **135**, 014112 (2011).
- [39] C. Hartmann, V.-M. Vulcanov, and C. Schütte, *Multiscale Modeling & Simulation* **8**, 1348 (2010).
- [40] C. Hartmann, B. Schäfer-Bung, and A. Thöns-Zueva, *SIAM Journal on Control and Optimization* **51**, 2356 (2013).
- [41] T. Breiten and T. Damm, *Systems & Control Letters* **59**, 443 (2010).
- [42] P. Benner and T. Breiten, *SIAM Journal on Matrix Analysis and Applications* **33**, 859 (2012).
- [43] M. V. Korolkov, G. Paramonov, and B. Schmidt, *The Journal of Chemical Physics* **105**, 1862 (1996).
- [44] R. Mecke, *Zeitschrift für Elektrochemie und angewandte physikalische Chemie* **54**, 38 (1950).
- [45] N. Owschimikow, B. Schmidt, and N. Schwentner, *Physical Chemistry Chemical Physics* **13**, 8671 (2011).
- [46] B. Schmidt and B. Friedrich, *The Journal of Chemical Physics* **140**, 064317 (2014).
- [47] J. I. Steinfeld, J. S. Francisco, and W. L. Hase, *Chemical Kinetics and Dynamics* (Prentice Hall, Englewood Cliffs, NJ, 1989).
- [48] R. S. Burkey and C. D. Cantrell, *Journal of the Optical Society of America B* **1**, 169 (1984).
- [49] M. Seel and W. Domcke, *The Journal of Chemical Physics* **95**, 7806 (1991).

- [50] K. Zhou and J. C. Doyle, *Essentials of Robust Control* (Prentice Hall, 1998).
- [51] I. Andrianov and P. Saalfrank, *The Journal of Chemical Physics* **124**, 034710 (2006).
- [52] K. Sundermann and R. de Vivie-Riedle, *The Journal of Chemical Physics* **110**, 1896 (1999).
- [53] C. Le Bris, Y. Maday, and G. Turinici, in *Quantum Control: Mathematical and Numerical Challenges : CRM Workshop*, edited by A. D. Bandrauk, M. C. Delfour, and C. Le Bris (American Chemical Society, 2003), p. 139.
- [54] J. Somló, V. A. Kazakov, and D. J. Tannor, *Chemical Physics* **172**, 85 (1993).
- [55] N. Khaneja, T. Reiss, C. Kehlet, T. Schulte-Herbrüggen, and S. J. Glaser, *Journal of Magnetic Resonance* **172**, 296 (2005).
- [56] L. Zhang and J. Lam, *Automatica* **38**, 205 (2002).
- [57] Z. Bai and D. Skoogh, *Linear Algebra and its Applications* **415**, 406 (2006).
- [58] E. L. Wachspress, *Applied Mathematics Letters* **1**, 87 (1988).
- [59] T. Damm, *Numerical Linear Algebra with Applications* **15**, 853 (2008).
- [60] A. Laub, M. Heath, C. Paige, and R. Ward, *IEEE Transactions on Automatic Control* **32**, 115 (1987).
- [61] M. S. Tombs and I. Postlethwaite, *International Journal of Control* **46**, 1319 (1987).
- [62] J. Hahn and T. F. Edgar, *Industrial & Engineering Chemistry Research* **41**, 2204 (2002).
- [63] I. Horenko, B. Schmidt, and C. Schütte, *The Journal of Chemical Physics* **117**, 4643 (2002).
- [64] I. Horenko, C. Salzmann, B. Schmidt, and C. Schütte, *The Journal of Chemical Physics* **117**, 11075 (2002).
- [65] I. Horenko, M. Weiser, B. Schmidt, and C. Schütte, *The Journal of Chemical Physics* **120**, 8913 (2004).
- [66] J. E. Subotnik, A. Jain, B. Landry, A. Petit, W. Ouyang, and N. Bellonzi, *Annual Review of Physical Chemistry* **67**, 387 (2016).
- [67] J. C. Tremblay, S. Klinkusch, T. Klamroth, and P. Saalfrank, *Journal of Chemical Physics* **134**, 044311 (2011).
- [68] D. M. Lockwood, M. Ratner, and R. Kosloff, *Chemical Physics* **268**, 55 (2001).

FIG. 1: Flow chart of the WAVEPACKET functions, also indicating the names of the files used for exchange of data between them. The left dashed red line indicates the border between the descriptions of quantum dynamics by partial differential equations (PDEs, using discrete variable representation) and by ordinary differential equations (ODEs, using energy representation). The right dashed red line marks the separation between quantum mechanics (QM) and dimension reduction and optimal control theory (OCT).

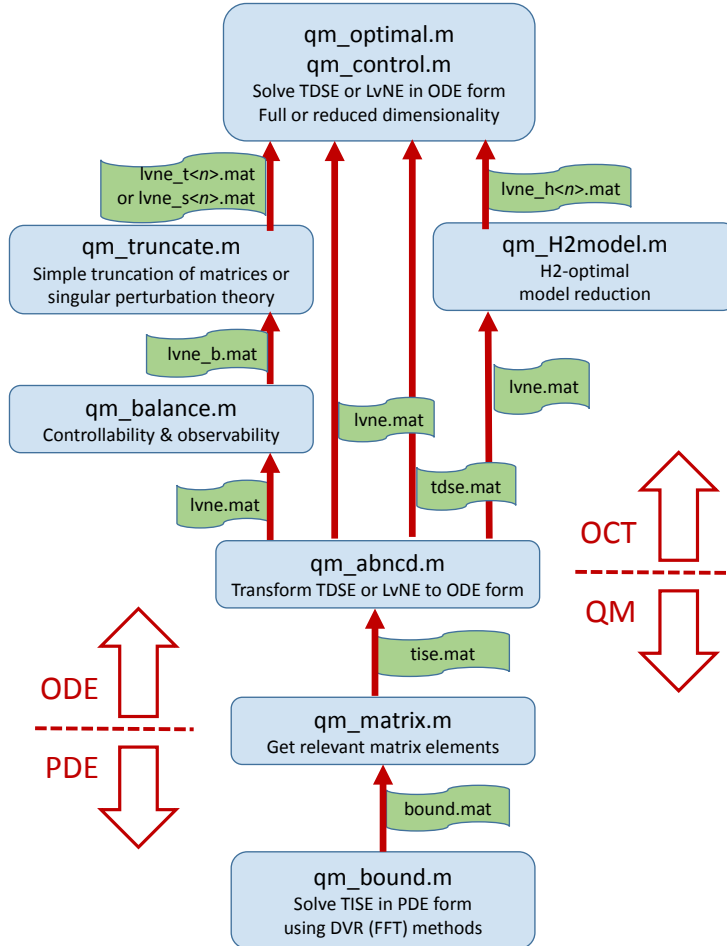


FIG. 2: Spectrum of the A matrix for the Morse oscillator of Ref. [43] (bound states only). The coupling to a thermal bath is described by a Lindblad model, using Fermi's golden rule (B3) for the relaxation rates. The matrix is generated using the WAVEPACKET function `qm_abncd`, assuming a relaxation rate $\Gamma_{0 \leftarrow 1} = 2 \text{ ps}^{-1}$ and temperature $\Theta = 0$.

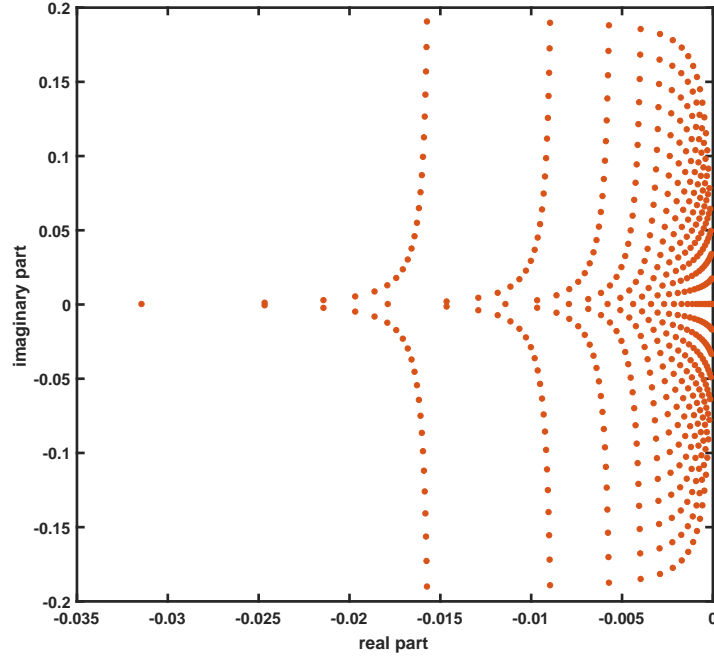


FIG. 3: Field-free population dynamics for the Morse oscillator of Ref. [43] during the first picosecond (ps). The coupling to a thermal bath is described by a Lindblad model, using Fermi's golden rule (B3) with relaxation rate $\Gamma_{0 \leftarrow 1} = 2 \text{ ps}^{-1}$ and temperature $\Theta = 0$. The evolution is simulated using the WAVEPACKET function `qm.control`, assuming the system initially to be in the $v = 5$ state. Note that 1 ps corresponds to 41,341 atomic units of time.

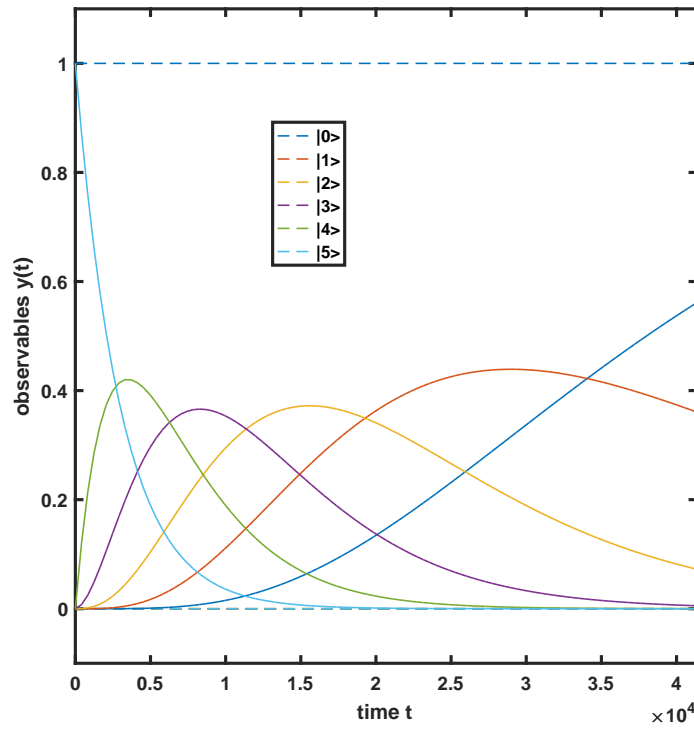


FIG. 4: Field-induced population dynamics for the Morse oscillator of Ref. [43]. The vibrational excitation with a strong infrared laser pulse during the first picosecond (ps), same as in Fig. 2 of part I, competes with the relaxation, same as in Fig. 3 here. The evolution is simulated using the WAVEPACKET function `qm_control`, assuming the system initially to be in the $v = 0$ state. Note that 1 ps corresponds to 41,341 atomic units of time.

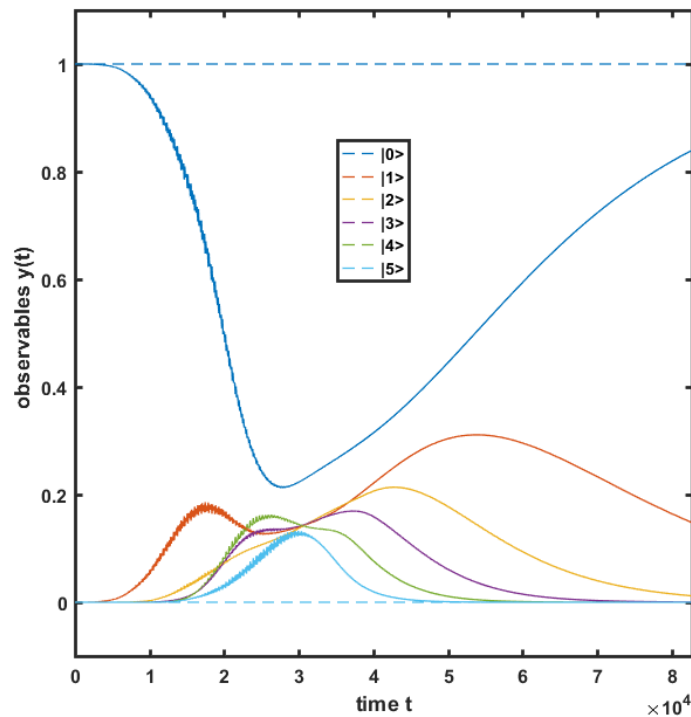


FIG. 5: Optimal control of population for the Morse oscillator of Ref. [43], using the WAVEPACKET function `qm_optimal`. From left to right: TDSE simulation for functional J_{1a} , LvNE for J_{1b} , TDSE for J_{1c} . Top to bottom: Control field $u(t)$, population dynamics $y(t)$, target functional $J_1(t)$, cost functional $J_2(t)$.

